Dr. Jordan Hanson
Assistant Professor of Physics and Computer Science
Whittier College
Whittier, California

One and Two Dimensional RF Phased Array Simulations with MIT Electromagnetic Equation Propagation (MEEP): Designs for Active Seeker Radar Verification and Testing

Abstract

Naval munitions involve active radar systems for target acquisition. In order to lay the groundwork for the construction of a system designed to probe existing active seeker radar systems, the MIT Electromagnetic Equation Propagation (MEEP) code was used to mode radio-frequency (RF) phased arrays in one and two dimensions. Phased arrays are sets of RF antennas that radiate and receive as coordinated units to enhance signal to noise ratio (SNR), form synthetic aperture radar (SAR). In this application, we seek to build a testing system that can probe and diagnose issues with existing active seeker radar, and phased arrays offer a flexible system that does not have to be moved in order to probe seeker radar off-axis. Further, phased arrays can be designed to work over a range of frequencies. Thus, a properly designed two-dimensional array of broadband antennas could probe active seekers off-axis in polar and azimuth angle at a variety of operating frequencies. MEEP was used to develop a prototype design, and the properties of the two and three-dimensional versions of the array are presented.

1. Introduction

The research into broadband RF two-dimensional phased arrays began through the discussion of techniques beneficial to "the support and testing of active RF ranging and positioning systems, where we expect the unit under test to use a monopulse transceiver system through an antenna array." Further, since "far field testing is often impractical," an RF transceiver system was needed to mimic off-axis reflections relative to the active seeker radar array[1]. In general, "phase shifting multiple RF inputs (one per array element)" has become a common method of generating plane waves a few wavelengths from a collection of RF transmitters, and "directional testing of radial antenna arrays" from active seekers is a straightforward application of this technique. In the field of RF-based high-energy neutrino detection, the linear phased array concept has become important for lowering the minimum detectable SNR of RF transient pulses created by extra-solar cosmic rays and neutrinos. Thus, there was a potential synergy between the engineering needs of the active seeker testing program at the Naval Surface Warfare Center, and the scientific research connected to Whittier College.

The coronavirus pandemic, however, forced adaptation in our research methods, which initially included building a system in the laboratory. We began to perform a standard academic literature review of phased array concepts in the multi-GHz bandwidth. However, we soon discovered that we could *design* the systems we would like to build eventually through simulations of the system performance with appropriate software. This *Monte Carlo* approach, design through simulation and comparison to relevant theoretical equations, is often used in the design of large high-energy physics detectors. Typically detectors like ARIANNA, ARA, ANITA, and IceCube-Gen2 that involve RF systems are designed using RF antenna modeling software. Often this software is expensive and proprietary. However, Maxwell's equations govern RF dynamics, just like any other electromagnetic system, so we selected a finite difference time-domain solver (FDTD) called the MIT Electromagnetic

1 Quotes are from original design planning discussions held at the outset of the 2020 summer program start.

Equation Propagation (MEEP) package. Written with an Anaconda/Python interface, this open-source software was deployed to model, element by element, a two-dimensional phased array with a full 3D CAD-like description of the RF antennas. By simulating the electric fields radiated from the antennas, with appropriate phase shifts for each antenna, we have created a working model of the phased array system we'd like to build. We remark in Sec. 2 on how the model works, and In Section 3 we show some preliminary results. Section 4 contains the conclusions.

2. One and Two-Dimensional Phased Array Systems

Consider a row of RF antennas pointed all in the same direction. If each receives the same voltage signal to radiate, the signals can be made to constructively interfere and form a powerful plane wave if the inter-antenna spacing was correct. The appropriate inter-antenna spacing is such that the distance d between antennas is comparable to the wavelength λ of the radiated signals. That is, $\lambda/d \sim 1$. Introducing a constant phase shift per antenna in the otherwise identical signals passed to each antenna in the row has the effect of forming a plane wave identical to the non-phase shifted case, but diverted by a *beam angle* relative to *broadside*, or the original direction. Introducing a different phase shift per antenna results in a different beam angle. For example, if three antennas were co-linear and given the same signals with phases of 0 degrees, 15 degrees, and 30 degrees, the constant phase shift per antenna would be 15 degrees. The beam angle depends on λ/d. If the constant phase shift per antenna were changed to 5 degrees per antenna, the beam angle would decrease by a factor of three, because the beam angle is proportional to the phase shift per antenna and λ/d. Thus, an active seeker under test could be placed in front of a phased array, sufficiently far from the array as to experience the plane wave behavior (mimicking the far-field).

Consider a two-dimensional grid of antennas now, with relative phase shift per *row* of antennas, and relative phase shift per *column*. Thus, the antenna labeled by (0,0) could have a phase of 0 degrees, and the antenna labeled by (n,n) in an $n \times n$ array could have the maximum phase shift. There are then *two* beam angles, one polar and one azimuth. In a grid of antennas, the polar and azimuth can be controlled independently by the row and column phase shifts. The *radiation pattern* is a function normalized to the maximum power radiated at the beam angle, versus the azimuth and polar angles. Often three-dimensional surfaces like the radiation patterns are summarized by two-dimensional graphs of characteristic planes cutting through the surfaces. In the case of linearly polarized antennas, two such planes are the E and H planes, corresponding to the plane containing the E-field vector and H-field vector, respectively. Our simulated models of the one-dimensional and two-dimensional phase array grids for active radar testing and verification are shown to agree with mathematical predictions from antenna array theory. Further, we employ two different array element types: Yagi-Uda antennas and dual-polarization horn antennas in our grids. While the former is used for single-frequency applications, the latter is meant to be a broadband solution.

3. Results

The one-dimensional Yagi-Uda array of $n = 16$ antennas is shown in Fig. 1 (left). The MEEP simulation requires definitions of the metal dipoles that comprise each antenna element (white), and the locations of the radiators (red). The blue box around the array records the flux of E and H at each point and extends them into the far-field. The array is fed continuous sine waves at frequencies near 5 GHz, with 60 degrees phase shift per antenna. The resulting radiation pattern is shown in Fig. 1 (right). The beam has a width of 5 degrees and is deflected away from *broadside* to the beam angle. Figure 2 shows the results for the beam angle versus phase shift. The result is a linear relationship, given by

$$\Delta\Phi = 2\pi\left(\frac{d}{\lambda}\right)(\theta - \theta_0) \quad (1)$$

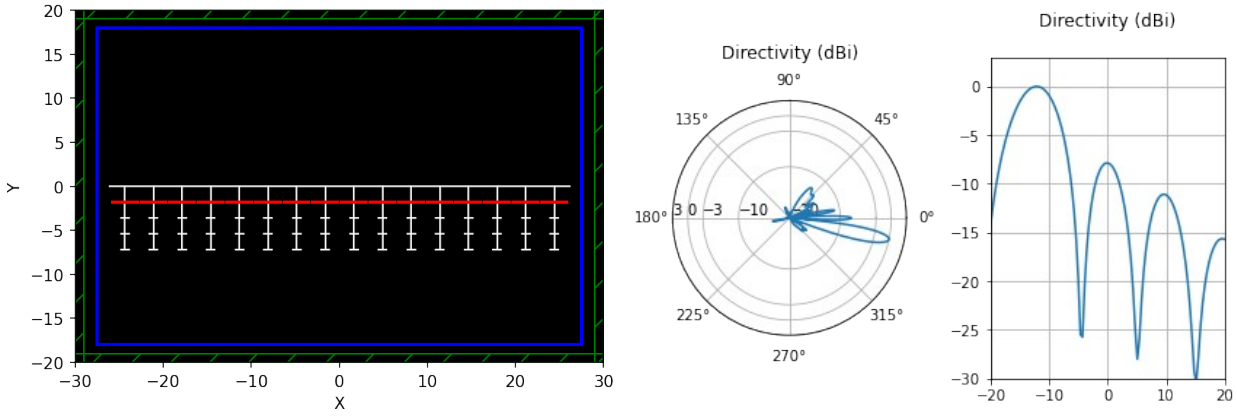

Figure 1. (Left) MEEP schematic of a *n = 16* element phased array at 5 GHz (Yagi-Uda elements). (Right) The radiation pattern (in power dB versus angle in both radial and Cartesian coordinates) has been steered by introducing a phase shift of 60 degrees per antenna.

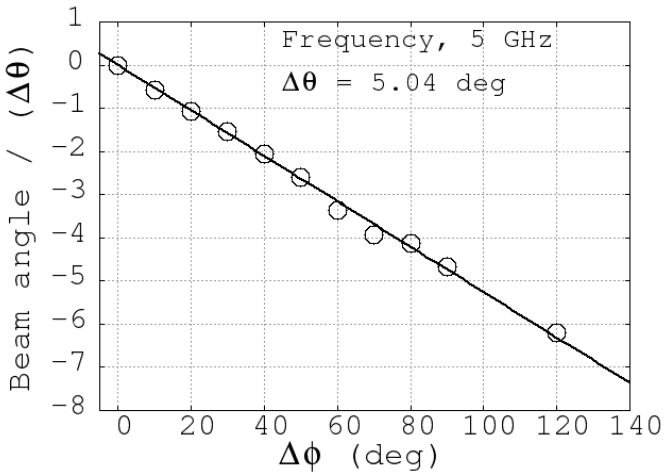

Figure 2. The beam width of the one dimensional Yagi-Uda array was 5.04 degrees, in agreement with the theoretical result (see Fig. xx). The angle, divided by the beam width is shown on the y-axis, versus the phase shift per antenna in degrees. The black line represents the mathematical prediction from array theory.

In Eq. 1, the left-hand side is the phase shift per antenna, and the right side shows the ratio of the inter-antenna spacing to the wavelength, times the shift in beam angle. Array theory also provides a (complex) expression for the radiation pattern given *n*, the number of antennas, the wavelength, the *d*, the inter-element spacing. Figure 3 (left) contains a comparison for the modeled *n = 16* Yagi-Uda array to the theoretical radiation pattern. Figure 3 (right) contains the result for generalizing to a two-dimension array of *16 x 16* antennas at 5 GHz. One-quarter of the 144 possible beam angles are shown. The number of possible beam angles is limited fundamentally by beam width, as the array must be steered by at least one beam width for the angle to be considered distinct. The relationship

between phase shift per antenna and beam angle in the two-dimensional Yagi array agrees with the theoretical prediction (Eq. 1) in polar and azimuth angle *separately* (Fig. 4).

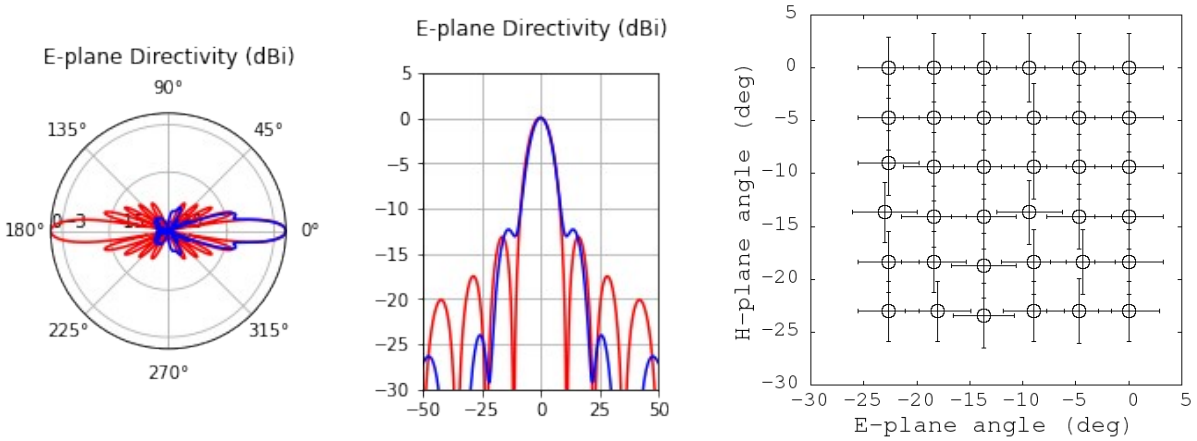

Figure 3. (Left) The theoretical radiation pattern at 5 GHz (red) agrees with the modeled radiation pattern (blue) for the Yagi array in the forward direction (0 degrees). The theoretical pattern is symmetric between forward and backward. However, real phased array systems are designed to have no backward lobes. (Right) Generalizing to a two-dimensional grid of antennas allows us to steer the beam to the 36 shown angles, one quadrant of the full 144 possibilities.

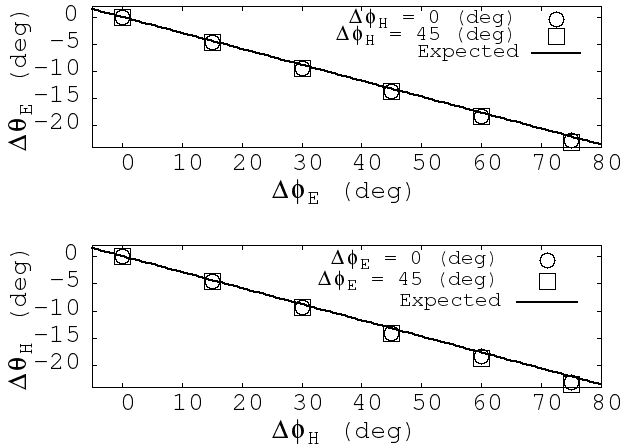

Figure 4. The E and H plane beam angles (divided by beam width) versus phase shift per *row* (top) and per *column* (bottom). The black lines are not fits, but purely theoretical predictions. In each plot, the circles and squares correspond to different phase shifts per antenna (0 and 45 degrees) in the *other plane*, implying that the phase versus angle relationships are *independent* in polar and azimuth.

In Fig. 5, we present a model of an RF *horn antenna*, meant to provide access to a range of frequencies rather than a single design frequency like the Yagi results. The simplest and clearest results arise from a two-dimensional simulation of a horn structure, and we later generalized to three dimensions. The exponential function describing the horn shape is shown in Fig. 5 (left) and the MEEP implementation is shown in Fig. 5 (right). A *n = 16* array of these two-dimensional structures was modeled and shown to agree with theory and obey beam steering (as in the Yagi-Uda case). Fig. 6. shows an example of a radiation pattern steered to three separate beam angles. Finally, in Fig. 7 we show results from generalizing the two-dimensional horn in Fig. 5 (right) to three dimensions, so that

we could create a *two-dimensional grid of broadband antennas*, constituting the full broadband phased array. Although deconstructive interference has not been fully eliminated, the 256 antennas are working together to form the main beam. This main beam can be steered in polar and azimuth angles, at a variety of frequencies. Although there is a backward lobe in the E plane, most likely caused by diffraction at the edges of our RF horns, the H plane is idea, with no side or backward lobes. The frequency must be lowered such that $\lambda/d \sim 1$, given the minimum inter-antenna element spacing from the horn geometry. This design will be further tuned and optimized to suit the probing of a wide variety of multi-GHz active seeker radars in an anechoic chamber setting.

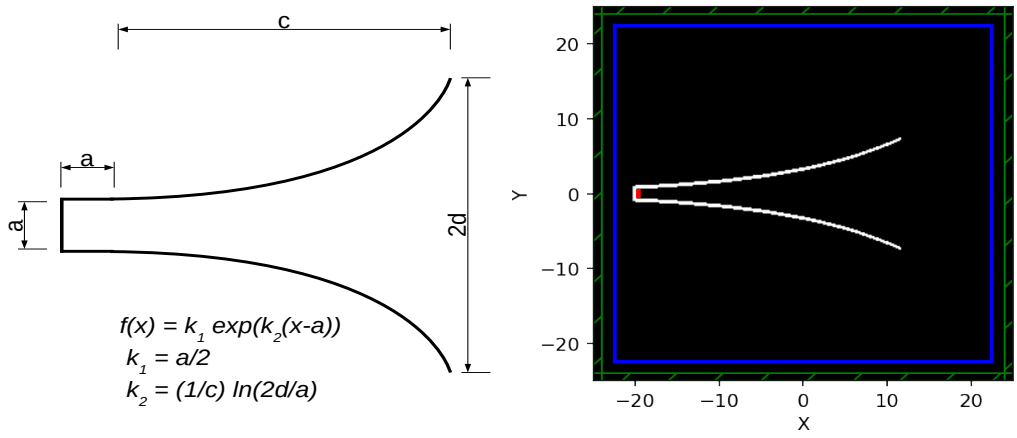

Figure 5. (Left) Three parameters *a*, *c*, and *d* describe the shape of the RF horn, with the radiator located at the small end. (Right) A two-dimensional implementation in MEEP of this horn.

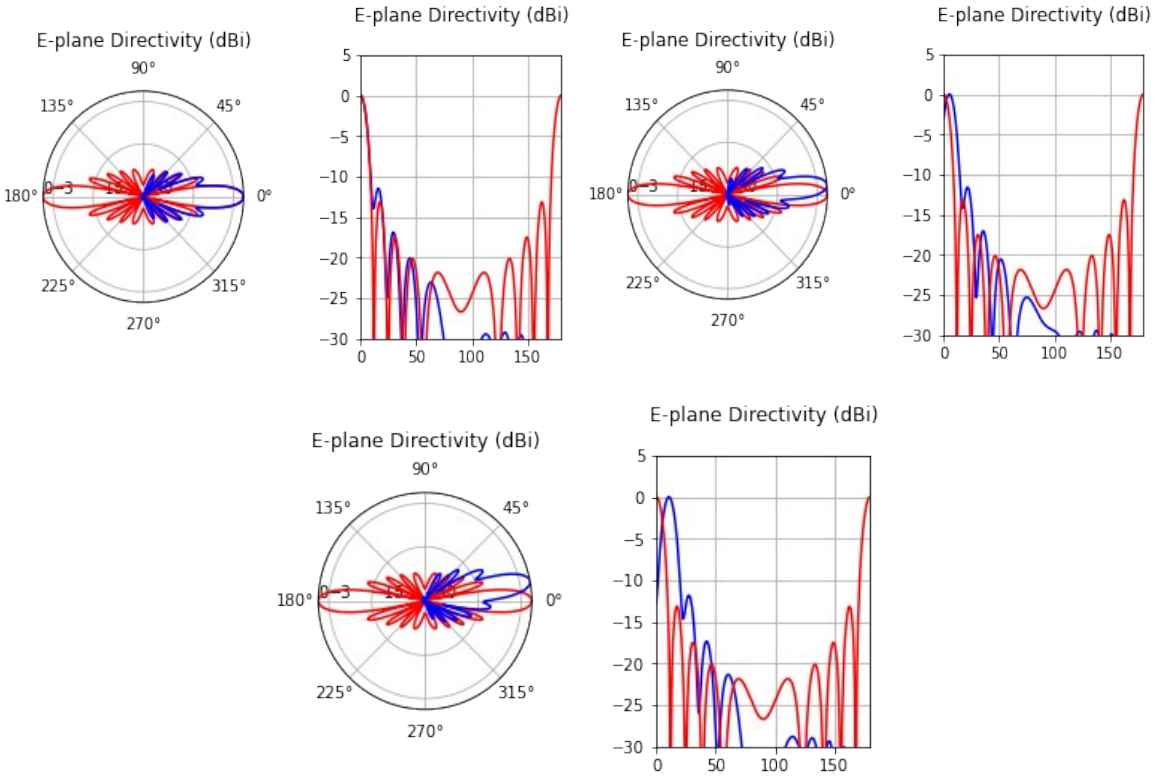

Figure 6. Results from *n = 16* one dimensional phased array of two-dimensional horns at 1.2 GHz. The array steered to the expected beam angle, and matched theoretical radiation patterns across a bandwidth from 0.3 to 3.0 GHz.

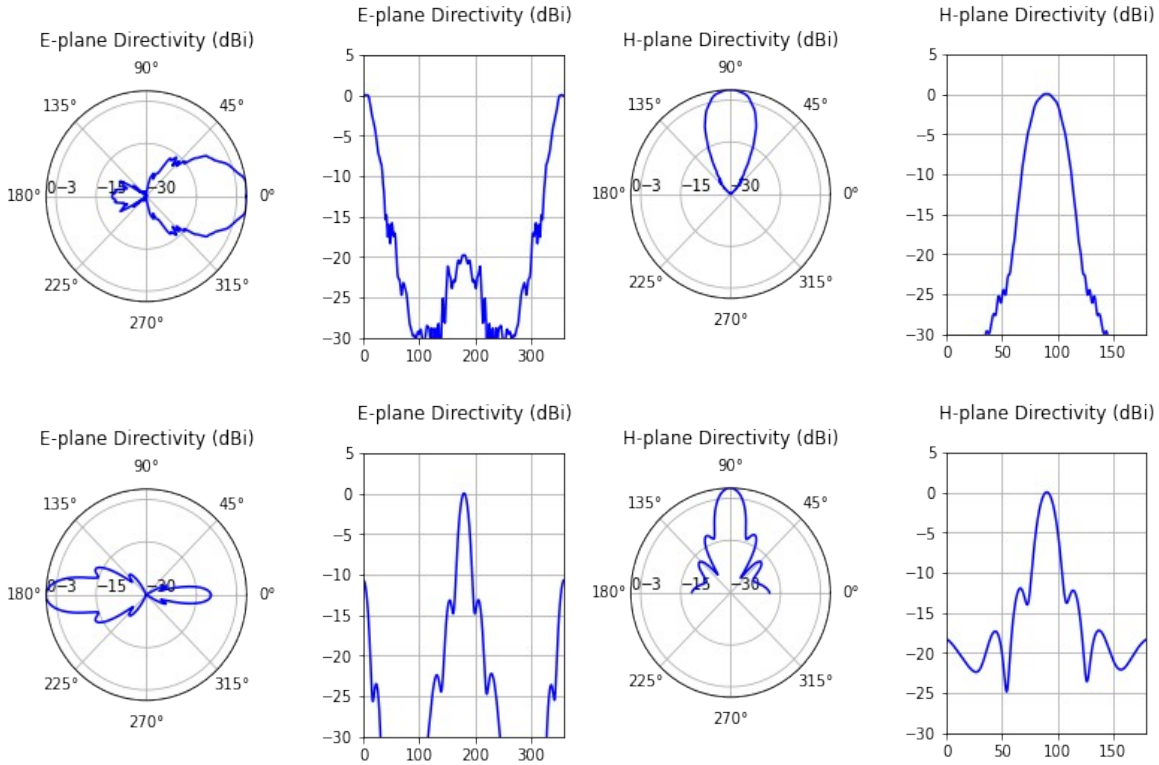

Figure 7. (Left, top) The E plane and (right, top) H plane of our three dimensional broad band RF horn designed to operate between 3 and 30 GHz. (Bottom, left) The E plane and (bottom, right) H plane of our *16 x 16* array of RF horns at 0.3 GHz, broadside beam angle (0 deg, 0 deg). Though there is a backward lobe in the E-plane, the H-plane is ideal.

4. Conclusions

We have concluded a broad study of narrowband and broadband phased array systems in one and two-dimensions, with the goal of developing a versatile active seeker radar probing and calibration system. The system will be suitable to a wide variety of active seeker systems for two reasons. We will have the ability to tune the angular resolution by changing the frequency, and the ability to scan off-axis without moving the array by introducing the phase shifts per row and column of the two-dimensional grid of antennas. The MIT Electromagnetic Equation Propagation (MEEP) package was used to successfully model phased array systems that can be practically constructed, while showing that the array results agree with theoretical derivations of radiation pattern, and shift in beam angle. We would like to acknowledge and thank the Office of Naval Research for their diligence in continuing this Summer Faculty Research Program despite the COVID-19 pandemic. We thank especially Gary Yeakley, Jeffrey Benson, Van Nguyen, and Golda McWhorter for their helpful insights during summer meetings. Future research in coordination with the Naval Surface Warfare Center will likely include constructing a model of this system for real radar testing, and the model will prove useful in design modifications.